

Catalytic Partial Oxidation of Ethane to Acetic Acid over $\text{Mo}_1\text{V}_{0.25}\text{Nb}_{0.12}\text{Pd}_{0.0005}\text{O}_x$

I. Catalyst Performance and Reaction Mechanism

David Linke,* Dorit Wolf,* Manfred Baerns,*¹ Olaf Timpe,† Robert Schlögl,‡
Sabine Zeyß,‡ and Uwe Dingerdissen‡

*Institute for Applied Chemistry Berlin-Adlershof, Richard-Willstätter-Str. 12, D-12489 Berlin, Germany; †Fritz-Haber-Institut, Faradayweg 4-6, D-14195 Berlin, Germany; and ‡Aventis Research and Technologies GmbH & Co KG, D-65926 Frankfurt a.M., Germany

Received December 6, 2000; revised July 12, 2001; accepted August 1, 2001

DEDICATED TO PROFESSOR BERNHARD LÜCKE ON THE OCCASION OF HIS 65TH BIRTHDAY

The oxidation of ethane to acetic acid was studied over the title catalyst at temperatures between 500 and 580 K and elevated pressures between 1.3 and 1.6 MPa. Since water is known to favour acetic acid formation water was considered as an important variable. For a comprehensive characterisation of the catalyst SEM/EDX, TEM/EDX, XRD, XPS, TPD, and TAP were applied. The catalytic experiments revealed a change in reaction mechanism with temperature. While a consecutive reaction scheme dominates at low temperatures with ethylene as intermediate leading to acetic acid, ethylene and acetic acid are mainly formed in parallel at high temperatures. The initial step for both pathways is the reaction of ethane with lattice oxygen; vanadium acts as redox centre. The ethylene formed undergoes a consecutive reaction to acetic acid which can be described as a heterogeneous Wacker-like reaction, where highly dispersed Pd(II) acts as a catalytically active centre. The role of water in this step seems to be similar to that in the homogeneous Wacker reaction of ethylene to acetic acid. The high dispersion of palladium in the present catalyst system maintained under reaction conditions results from the incorporation of small amounts of palladium into a Mo_5O_{14} like phase serving as host structure also for vanadium and niobium. © 2002 Elsevier Science

Key Words: selective oxidation; ethane; acetic acid; ethylene; heterogeneous Wacker oxidation; mechanism.

1. INTRODUCTION

Acetic acid is one of the most important chemical products with a worldwide demand of about 5.4 million tons in 1997 (1). In 2000, a global total capacity of 8.36 million and a supply of 6.35 million tons/year are expected which corresponds to an average annual growth rate (1997–2002)

¹ To whom correspondence should be addressed. E-mail: baerns@aca-berlin.de. Fax: +49 30 6392-4454.

of 3.4%. Since the discovery of a new iodide-promoted rhodium catalyst with remarkable activity and selectivity for methanol carbonylation by Monsanto researchers in 1968 this process has become the dominating technology for the production of acetic acid (ca. 60% of total capacity) (2). Only a minor proportion is produced by liquid phase hydrocarbon oxidation (10%: n-butane, naphtha), by ethylene oxidation (25%), and by fermentation of carbohydrates (5%). Although there is presently no economic alternative to the Monsanto process, a highly selective direct oxidation of ethane to acetic acid might become attractive since ethane is available at low costs as the second major component of natural gas (3–20 mole-%) (3). Moreover, all methanol carbonylation processes suffer from high investment costs, due to zirconium-lined equipment, which is the preferred material of construction because of corrosion problems. Additionally, all carbonylation processes need an iodide source as co-catalyst. Traces of iodide in acetic acid could lead to catalyst poisoning problems in some downstream applications such as in vinyl acetate manufacture (major end use product), and therefore has to be costly removed. Thus, a technology such as the direct partial oxidation of ethane which avoids these problems might be an economical alternative.

The pioneering work in ethane oxidation to acetic acid goes back to Thorsteinson *et al.* (4) who studied Mo-V mixed oxide catalysts containing an additional metal oxide. The catalyst of the composition $\text{Mo}_1\text{V}_{0.25}\text{Nb}_{0.12}\text{O}_x$ showed the highest activity and selectivity to ethylene in the temperature range from 473 to 673 K. The authors found that at atmospheric pressure ethylene was the only product besides CO_x . At a total pressure of 2.1 MPa acetic acid was formed with selectivities up to 26% ($T = 593$ K). Kinetic experiments carried out in a Berty reactor with the same

catalyst suggested a consecutive reaction scheme for the formation of acetic acid with ethylene as the intermediate product. The rate of the oxidation of ethylene to acetic acid is accelerated by water. Carbon monoxide as well as carbon dioxide were exclusively formed by oxidation of ethylene. A redox mechanism with molybdenum as active centre was suggested assuming an ethoxy species as intermediate in ethylene formation. According to Thorsteinson *et al.* (4) the role of vanadium and niobium is both to stabilise the catalytically active phase and to enhance reoxidation of Mo^{IV} to Mo^{VI} . The formation of acetic acid over $\text{Mo}_1\text{V}_{0.25}\text{Nb}_{0.12}\text{O}_x$ was confirmed by other groups (5–7). Merzouki *et al.* (5) found acetic acid even at atmospheric pressure provided that the catalyst was prepared in hydrochloric acid leading to the formation of a Mo_5O_{14} phase together with MoO_3 . In contrast, catalyst preparation in oxalic acid led to the formation of $\text{Mo}_{18}\text{O}_{52}$. In this case, no acetic acid formation could be observed. Since a relationship between the presence of Mo_5O_{14} and acetic acid formation was noticed the authors proposed a model of active Mo_5O_{14} sites in MoO_3 .

Further studies showed that it is still not clear whether the molybdenum or vanadium cation forms the active centre for acetic acid production. Merzouki *et al.* (5) and Ruth and colleagues (6, 7) studied MoO_x and MoNb_xO_y catalysts without vanadium and reported that none of these catalysts were active for ethane oxidation to acetic acid. On the other hand, it was shown that VO_x and VPO are active for acetic acid formation (5, 8–10). Tessier *et al.* (9) assigned acetic acid formation to vanadate dimers or plyvanadates respectively, as indicated by IR studies on supported VO_x and VPO catalysts. Obviously, the formation of acetic acid depends on the presence of vanadium which makes vanadium more likely to form the catalytically active centre, particularly since catalysts based on MoO_x or MoNb_yO_x could not form acetic acid from ethane. This essential role of vanadium is confirmed considering other catalytic systems for oxidising ethane to acetic acid which always contains vanadium as reported in the patent literature. Accordingly, active catalysts were derived from Mo-V-Nb- O_x by replacing Mo with Re and/or W (11–13), and by adding Re to VPO catalysts (14).

Merzouki *et al.* (5, 8) reported that doping VO_x with palladium enhances the selectivity to acetic acid; similar results were obtained by doping VPO with palladium (5, 8). Recently Borchert *et al.* (15–17) showed that the positive effect of palladium can be used to obtain highly selective catalysts for the production of acetic acid. For a catalyst having the stoichiometric composition $\text{Mo}_1\text{V}_{0.25}\text{Nb}_{0.12}\text{Pd}_{0.0005}\text{O}_x$, which is, apart from palladium, close to the original MoVNbO catalyst studied by Thorsteinson *et al.* (4), highly improved selectivities to acetic acid were observed: at 553 K and a total pressure of 1.5 MPa the selectivity to acetic acid was 78% at 10% ethane conversion with palladium but only 32% at 9% ethane conversion without palladium

(15). In two other patents Borchert *et al.* mentioned that palladium also strongly improves the selectivity to acetic acid of ReVNbO catalysts (16) and of WVNbO catalysts (17), which were patented without palladium as an essential component by Kitson (12, 13) and Hallet (11), respectively.

The role of palladium has not been understood until now. Results of Borchert *et al.* (15) for $\text{Mo}_1\text{V}_{0.25}\text{Nb}_{0.12}\text{O}_x$ and $\text{Mo}_1\text{V}_{0.25}\text{Nb}_{0.12}\text{Pd}_{0.0005}\text{O}_x$ show that the addition of palladium increased the selectivity to acetic acid at the expense of ethylene selectivity. For the conversion only a slight increase was found in the presence of palladium.

Since the oxidation of ethylene to acetic acid is a part in the reaction scheme suggested by Thorsteinson *et al.* (4), we want to point out some aspects of this reaction. In the homogeneous oxidation of ethylene to acetaldehyde, known as Wacker oxidation, a Pd(II) complex is used as catalyst in the presence of Cu(II) as co-catalysts. The heterogeneous analogue of the Wacker oxidation is performed over redox catalysts such as V_2O_5 or heteropoly acids doped with small amounts of palladium (18–21). As in the homogeneous Wacker reaction palladium is the only metal known which catalyses the heterogeneous Wacker oxidation effectively. One difference to the homogeneous reaction is that acetic acid is formed as the main product with increasing temperature instead of acetaldehyde, which is very sensible to deep oxidation. A positive effect of water on activity as well as selectivity was observed (19, 20, 28). Two different mechanistic ideas have been reported to explain the accelerating effect of water. Seoane *et al.* (19) considered that water accelerates the desorption of acetic acid and acetaldehyde. The second explanation for the accelerating effect of water considers hydroxyl groups as essential constituents of the catalytically active centre, which was first used by Evnin *et al.* (18) in 1973 and was later adopted to heterogeneous Wacker oxidation on Cu/Pd exchanged Y-zeolites (22). Strong support for the second approach considering hydroxyl groups as constituent of the active centre is given by Van der Heide *et al.* (20) who showed that the rate of acetaldehyde formation in the oxidation of ethylene is proportional to the amount of adsorbed water, which was separately determined by measuring the adsorption isotherms of water on the catalyst.

In the present study, we have investigated the oxidation of ethane to acetic acid over a $\text{Mo}_1\text{V}_{0.25}\text{Nb}_{0.12}\text{Pd}_{0.0005}\text{O}_x$ catalyst (15). The catalyst was chosen for its high activity and selectivity as well as its superior long-term stability compared to rhenium containing catalysts. Moreover, this catalyst can be considered as a representative for the new Pd-containing systems described in patent literature. The first aim of this study was to elucidate the role of the catalyst components (Mo, V, Nb, and especially Pd). For a comprehensive study of the catalyst various techniques were applied (scanning electron microscopy/energy dispersive X-ray analysis (SEM/EDX), X-ray diffraction (XRD),

temperature programmed desorption (TPD) of ethane, temporal analysis of products, and temperature programmed reaction spectroscopy). The second aim of this study was to find out the influence of operating conditions on catalyst performance (i.e., ethane conversion and acetic acid selectivity) under close-to-practise conditions. A steady-state fixed-bed reactor was used at elevated pressures of 1.2 to 1.6 MPa. The role of water was particularly taken into consideration since a beneficial influence of water was reported for the formation of acetic acid (4, 9). The results of both fundamental and close-to-practise experiments were used to obtain information on the mechanism of the oxidation of ethane to acetic acid. In the second part of the series (23) we use the present data as basis for deriving the kinetics of the title reaction.

2. EXPERIMENTAL

2.1. Catalyst

$\text{Mo}_1\text{V}_{0.25}\text{Nb}_{0.12}\text{Pd}_{0.0005}\text{O}_x$ used as catalyst was prepared according to the procedure described in (15). Three aqueous solutions were used (a) 10.20 g ammonium vanadate was solved in 25 ml of water, (b) 27.51 g niobium oxalate in 25 ml of water, and (c) 61.75 g ammonium molybdate plus 39 mg palladium acetate in 200 ml of water. After each solution was stirred separately at 363 K for 15 min the niobium containing solution was mixed with the vanadate solution and stirred again for 15 min at 363 K before adding the third solution. The mixture was stirred for additional 15 min at 363 K. The water was then evaporated and the resulting paste was dried for 16 h at 393 K. The solid was broken up and calcined for 4 h in static air at 673 K.

The BET surface area of the catalyst amounted to $9.3 \pm 0.2 \text{ m}^2/\text{g}$ after calcination. Particles of the sizes between 350 and 600 μm were used in the catalytic experiments.

2.2. Catalyst Characterisation Techniques

Scanning electron microscopy and energy dispersive X-ray analysis. SEM images were taken on a HITACHI S 4000 FEG microscope. EDX analysis was carried out using the EDAX DX-4 analysis system. An acceleration voltage of 15 kV was used; therefore, the depth of information is about 1 μm . With respect to the average particle size in the μm range, the results represent the bulk composition.

Transmission electron microscopy and energy dispersive X-ray analysis (TEM/EDX). For transmission-electron-microscopy a Philips CM200 apparatus was used. The sample was placed on a carbon grid. The electron energy for EDX-mapping was 200 keV.

X-ray diffraction. The powder X-ray diffraction measurements were carried out on a STOE Stadi P diffractometer in transmission geometry using Cu-K(α)-radiation.

XPS. XPS characterizations were carried out on a Leybold-Hereaus setup, equipped with a concentric hemi-

spherical detector, using Mg-K(α)-radiation. The movable sample holder allowed high temperature and high pressure treatment of the sample in reactive atmosphere. Measurements were done with the sample as is and after four successive treatments (i) 1 h, 523 K, 100 kPa, 100% oxygen; (ii) 1 h, 523 K, 10 kPa, 25% ethylene, 75% oxygen; (iii) 1.5 h, 623 K, 100 kPa, 25% ethylene, 75% oxygen; (iv) 1.5 h, 623 K, 100 kPa, 50% ethylene, 50% oxygen.

The spectra were background corrected and fitted by functions with a Gauss to Lorentz ratio of 1:1.

Temperature programmed desorption. A sample of 100 mg of the catalyst fixed by glass wool in the isothermal zone of a glass tube reactor was first heated in a nitrogen stream to 670 K to desorb water, and subsequently cooled to room temperature. Ethane adsorption was performed with 5% ethane in nitrogen (100 ml/min) for 5 min. Immediately after the adsorption, as soon as the nitrogen flow was free of ethane, the sample was heated at 5 K/min.

2.3. Transient Techniques for Mechanistic Studies

Temperature programmed reaction spectroscopy (TPRS). The TPRS-measurements were performed at 100 kPa with a tubular glass reactor of 7.5-mm inner diameter. The sample, usually 20 mg, was fixed at the isothermal zone by quartz wool. The total gas flow was set at 110 ml/min. The heating rate was set to 5 K/min. For ethane oxidation the feed composition was 10% ethane and 10% oxygen in nitrogen, for ethylene oxidation 5% ethylene and 20% oxygen in nitrogen.

All gases were used as delivered (Linde) without further purification. Gases were regulated and mixed with mass-flow controllers (Bronkhorst). Gas analysis was carried out by an IMR-MS (Atomika), allowing the discrimination by ionisation energy and the diminution of fragmentation. The quantification of major components was based on benzene as internal standard added to the off gases after the catalytic reactor.

Pulse experiments in the transient-analysis-of-products (TAP) reactor system. Pulse experiments were carried out in a temporal analysis of products reactor (TAP-2 reactor system) described elsewhere (24). The catalyst ($m_{\text{cat}} = 210 \text{ mg}$) was packed between two layers of quartz of the same particle size. Before the experiment the catalyst was treated with oxygen at 573 K. Then the reactor was evacuated at this temperature to 10^{-4} Pa for 20 min before a gas mixture was pulsed over the catalyst. A pulse contained approximately $2 \cdot 10^{15}$ molecules. The curves shown consists of the averaged responses of 10 pulses. It was assured that the catalytic performance and thus the pulses remain unchanged for many pulses.

2.4. Close-to-Practise Catalytic Testing

Feeding, reactor, and analysis. A flow sheet of the experimental set-up for the catalytic tests is shown in Fig. 1.

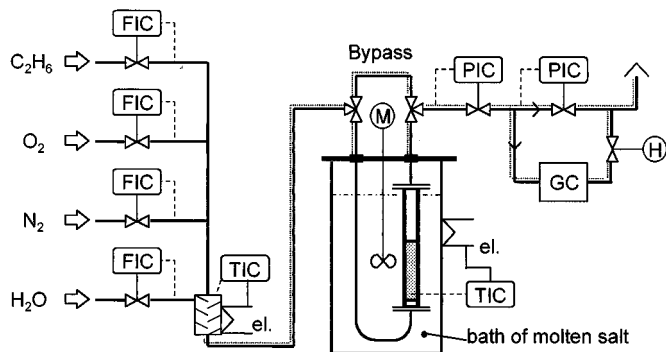


FIG. 1. Flowsheet of experimental set-up.

The gases as well as liquid water were fed by mass flow controllers (Bronkhorst). The purity of the gases used was for ethane 99.5%, for oxygen 99.995%, for nitrogen 99.999%, and for ethylene 99.7% (gas supplier Messer Griesheim). In the experiment with acetic acid added to the feed, a liquid mixture of water and acetic acid (Riedel-de Haën, >99.8%) was fed by the liquid mass flow controller. A heated mixer was used to evaporate the liquid and to mix it with the other gases. All subsequent transfer lines and valves were heated to 140°C in order to avoid condensation and adsorption. The feed gas mixture was either passed through the bypass or to the stainless steel tubular reactor (ID = 12 mm). The reactor was heated or cooled respectively by a stirred bath of salt ($\text{LiNO}_3/\text{KNO}_3/\text{NaNO}_3$). The axial temperature profile in the catalyst bed was measured by a NiCrNi-thermocouple inserted in a steel capillary (diameter = 2 mm). A mechanic back pressure controller was used to adjust reaction pressure. The second back pressure controller was set to 100 mbar and served the purpose of constant sample loop pressure in the online gas chromatograph (HP 5890 Series II). Separation of the components N_2 , O_2 , CO (plus traces of CH_4) was achieved using a molecular sieve 5-Å capillary column; CO_2 , H_2O , C_2H_4 , C_2H_6 , HOAc (and further trace products) were separated by a Poraplot Q capillary column. The effluent of both columns was combined and connected to a TCD and FID in series. Because of complete detection of all products (including water) balances of carbon, hydrogen, and oxygen could be calculated which were usually better than 98%.

Reactor operation and conditions. The reactor was operated as fixed bed. Nitrogen was used as the internal standard. In the present work the space-time is given as modified space-time τ_m which was calculated as mass of catalyst (m_{cat}) divided by the volumetric flow of feed gas at reaction temperature and pressure. All experiments were carried out with catalysts taken from the same charge. Deactivation of the catalyst was not observed during experimental runs (up to 50 h) which is in accordance with patent literature (15). The catalyst particles were diluted with twice the amount of quartz of the same size to achieve nearly isothermal operation. Reactions in the gas phase or reactions due to quartz

can be neglected, since preliminary experiments showed that ethane, ethylene, and acetic acid are not converted in the quartz-filled reactor under the reaction conditions used in the oxidation of ethane.

The oxidation of ethane was investigated in the temperature range from 503 to 576 K, at a total pressure range from 1.2 to 1.6 MPa, and at a total standard gas flow range from 1.5 to 11 $\text{ml} \cdot \text{s}^{-1}$. The catalyst mass was varied between 1 and 13.7 g. The feed gas contained ethane as the main component in stoichiometric excess (40 to 50% (v/v) ethane, ratio $\text{C}_2\text{H}_6/\text{O}_2 = 5$). The influence of water was studied by varying the water content between 0 and 20% (v/v).

The oxidation of ethylene to acetic acid was studied under conditions similar to those of the oxidation of ethane. In particular, water and oxygen partial pressures were in the same range. A low ethylene partial pressure was applied which corresponds to ethylene partial pressure found in the oxidation of ethane. Further experiments with co-feed of a reaction product, ethylene as well as acetic acid, were performed to study the influence of products on the conversion of ethane or its activity for unselective oxidation to carbon oxides. In these experiments, conditions similar to those in the oxidation of ethane were used. The exact conditions are given with the results.

3. EXPERIMENTAL RESULTS

3.1. Fundamental Studies

Phase composition and morphology of the catalyst. According to SEM/EDX (Figs. 2 and 3), TEM/EDX (Fig. 4), and XRD (Fig. 5), the catalyst sample contains crystals (maximum size 10 μm) that are mainly composed of Mo_xO_y , and less well-crystallised particles. The material shows two different morphologies (Fig. 2). The first species exhibits a crystalline, needlelike habit (area 1). These

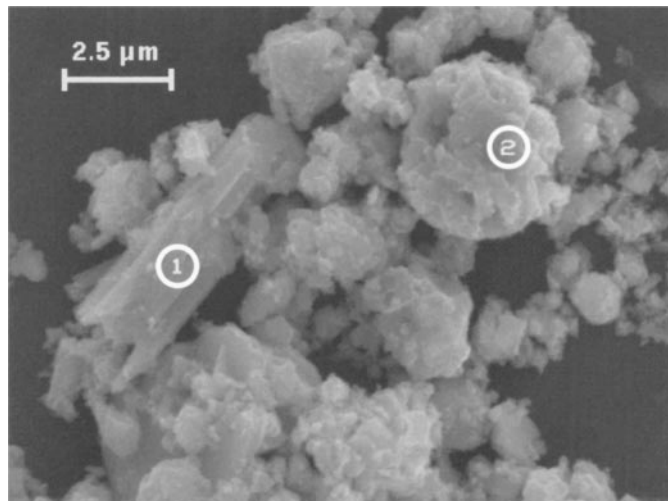


FIG. 2. SEM image of a fresh catalyst sample. The elemental composition was determined by EDX (15 kV) at the labelled points 1, 2.

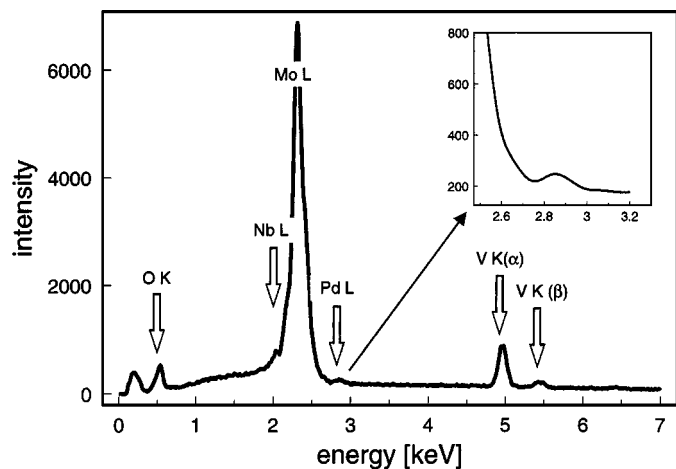


FIG. 3. SEM/EDX—spectrum of the catalyst recorded with excitation energy of 15 keV; in the insertion: zoom of the Pd L peak.

crystals have sizes of a few μm . The second type is described by very small particles with a lack of large and well-defined planes (area 2). The SEM/EDX analysis revealed a heterogeneous distribution of the main components (Mo, V, Nb). The needlelike large particles (at spot 1) are

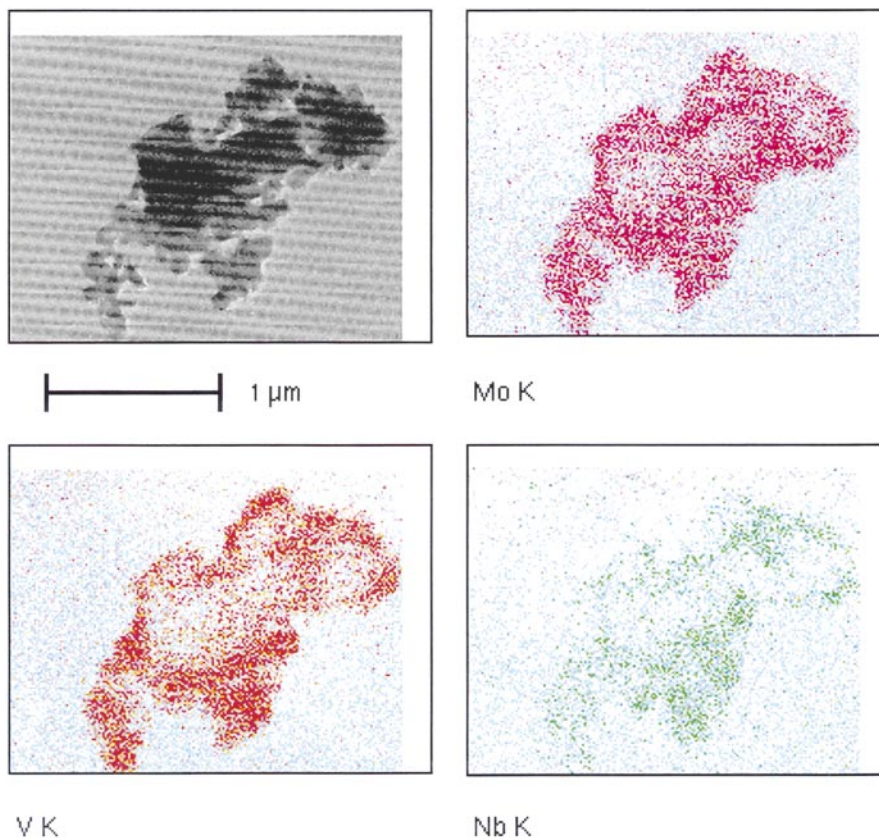


FIG. 4. TEM/EDX characterisation of the untreated catalyst; the distribution of the main constituents Mo, V, and Nb is shown by the intensity of the K-lines.

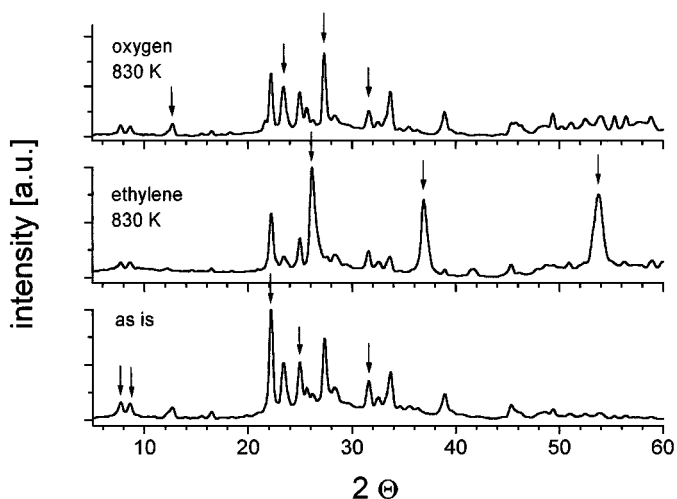


FIG. 5. XRD: Bottom: catalyst sample as is; middle: sample after reduction in (30%) ethylene atmosphere at 830 K; top: sample after calcination in (30%) oxygen atmosphere at 830 K. The most prominent reflections for the phases Mo_3O_{14} (bottom), MoO_2 (middle), and MoO_3 (top) are indicated.

significantly poorer in V than the surrounding matrix (at spot 2). For the former, an atomic ratio Mo/V of about 20 was found, whereas it was about 5 for the point labelled 2. The second ratio is much closer to the theoretical composition of the catalyst (Mo/V = 4). Moreover, the needlelike particles did not contain Nb above the detection limit of the method. The SEM/EDX palladium signal was near the detection limit (Fig. 3). XRD revealed that the catalyst is mainly composed of MoO_3 and Mo_5O_{14} , beside a pronounced amorphous fraction (Fig. 5). In particular, reflections of pure V- or Nb-oxides could not be detected. Since the Mo_5O_{14} structure is well known to be tolerant towards partial substitution by vanadium or niobium the occurrence of mixed phases according to the formula $\text{Mo}_{5-x}(\text{V/Nb})_x\text{O}_{14}$ can be assumed.

For more detailed information on elemental distribution TEM/EDX was applied (Fig. 4). Contrary to SEM/EDX palladium could not be detected. The regions at the bottom on the left-hand side of Fig. 4 (small needles) are characterised by a lack of vanadium and niobium. The shape of these crystallites corresponds to that of MoO_3 . Summarising, the results of microscopic principally show the nonhomogeneous morphology and elemental distribution.

The elemental composition of the surface was analysed by XPS (Fig. 6) applying the empirical sensitivity factors of elements. The surface composition remained unchanged during the different treatments by oxygen and ethylene/oxygen mixtures. A significant enrichment of vanadium was observed on the surface, whereas the concentration of niobium is below the nominal catalyst composition. The low surface concentration of niobium and bulk composition might result from the low solubility of the ni-

bium oxalate in water used as precursor component during preparation. As a consequence of the preferred niobium precipitation, it should be located preferably in the core of the particles.

The XPS spectrum of Mo(3d) does not show a significant change during the subsequent treatment steps (Fig. 7a). Molybdenum remains in its oxidation state (VI) even in the presence of ethylene (treatment steps 2 to 4). The Nb(3d) signal was not influenced by the catalyst treatment as well (not presented). The corresponding XPS spectra of V(2p) are shown in (Fig. 7b). The subsequent treatment steps lead to a change of the signal shape; at lower binding energy a shoulder occurs due to exposure to ethylene, which can be attributed to a partial reduction of V(V) to V(IV). The contribution of V(IV) and V(V) was analysed by least squares fit, as illustrated in Fig. 8a for the sample as received and after treatment step 4. The relative amount of V(IV) after the subsequent treatment steps is shown in Fig. 8b. The fraction vanadium in the oxidation state IV increases from about 4–5% after pure oxygen treatment (step 1) to 22% after exposure to reaction atmosphere (step 4). This trend does clearly indicate that the partial reduction of vanadium is not due to beam damages. The peaks of the Mo(3d) and the Nb(3d) signals could be fitted for all spectra assuming only the highest oxidation level for these elements.

Analysis of palladium appears to be difficult since the Pd(3d) signal is closed to the detection limits of the method (Fig. 9). The formation of a very weak signal was observed after treatment step 4 centered around a binding energy of 337.5 eV. This energy indicates the presence of Pd(II); no proof for the presence of metallic palladium can be found. The fact that the XPS signal arises only after the treatment

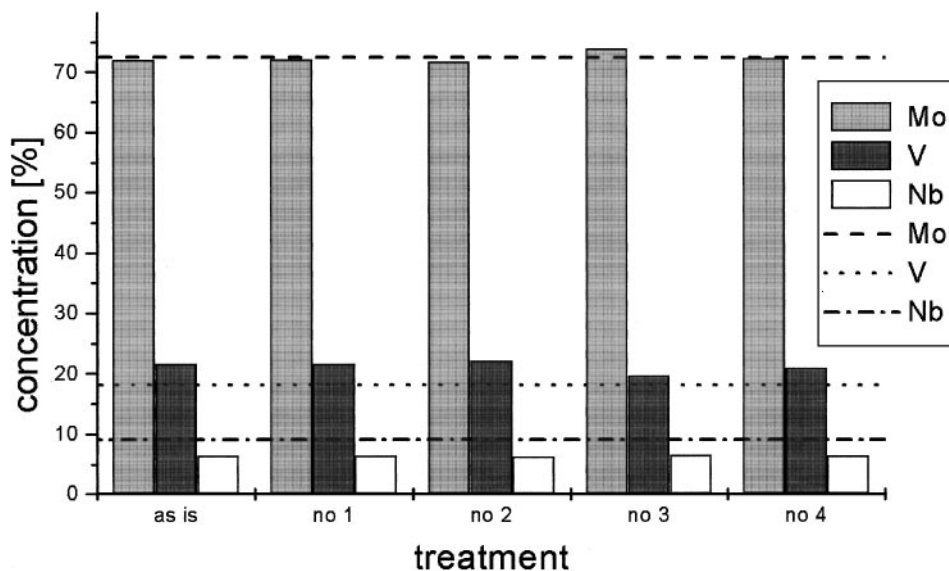


FIG. 6. Calculated sample composition based on least squares fits of the Mo (3d 5/2), V (2p 3/2), and Nb (3d 5/2) peaks; from left to right: untreated sample and after subsequent treatments (see Experimental section); the dashed lines indicate the overall sample composition.

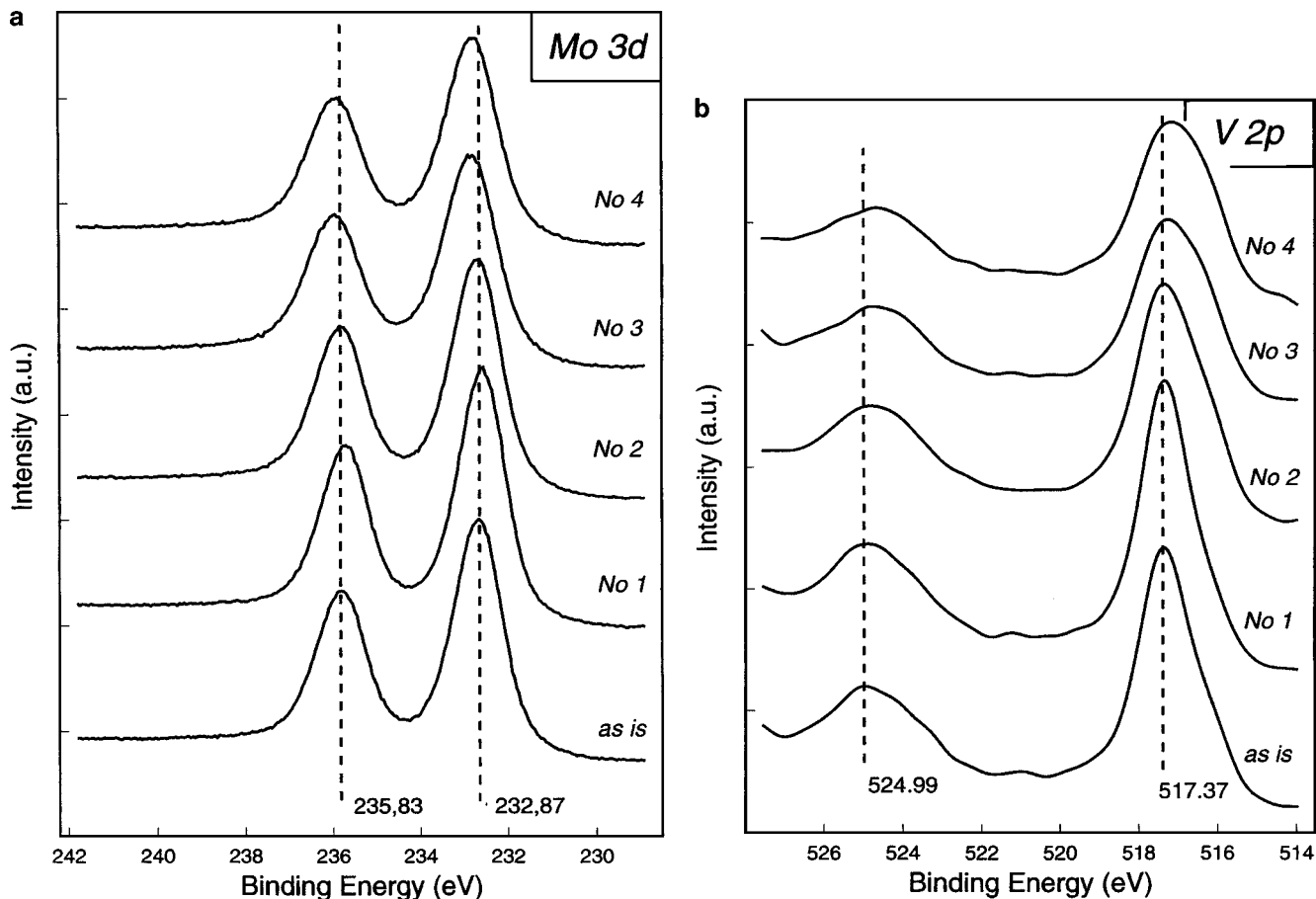


FIG. 7. XPS results after subsequent treatments (see Experimental section): (a) Mo (3d) signal of the catalyst and (b) V (2p) signal of the catalyst.

steps is probably related to a migration of palladium from the bulk to the surface.

Interaction between gas-phase reactants and catalyst.

Experimental results of TPRS of ethane and ethylene oxidation are shown in Fig. 10. At atmospheric pressure, the conversion of ethane and ethylene is very low and did not exceed 1% even at the highest temperatures applied. Only water, carbon dioxide, and acetic acid were the detected products. Other possible reaction products were below the detection limit. In the case of the ethane TPRS, the pronounced interference of the ethylene signal with the (feed) ethane signal prevented the detection of this possible product. The ethane TPRS is characterised by at least two steps (the first maximum in the water signal is attributed to release of moisture). At a rather low temperature, the catalyst showed a very small (note the multiplication factor) but distinct activity for acetic acid formation. The evolution of water and carbon dioxide simultaneously starts together with the acetic acid production and remains on a constant level up to about 600 K. Above this temperature, the water and carbon dioxide evolution rises approximately exponentially

with the temperature, as expected from thermodynamics. Compared to the ethane-TPRS, the ethylene-TPRS appears simpler. Here, the yields increase monotonously with temperature for all products. Acetic acid is simultaneously produced with water and carbon dioxide over the whole temperature range. The yield of acetic acid is at least one magnitude higher in the ethylene-TPRS than in the ethane-TPRS. Above 600 K, the slope of the ethylene-TPRS curves levels off, although the conversion is still below 1%. The reason is assumed an alteration of the catalyst. This deactivation was confirmed by a lower activity in a second TPRS-run (not shown).

The interaction of the gaseous substrate with the catalyst surface is of basic importance for the reaction mechanism. The sorption of ethane on the catalyst surface was investigated at atmospheric pressure (Fig. 11). The desorption starts with the beginning temperature ramp; ethane is completely desorbed at 500 K. The admixture of oxygen to the carrier gas (nitrogen) at maximum temperature (670 K) did not produce carbon oxides. A total amount of 3.23 μmol of desorbed ethane is calculated from the integral desorption peak. Assuming a spherical ethane molecule

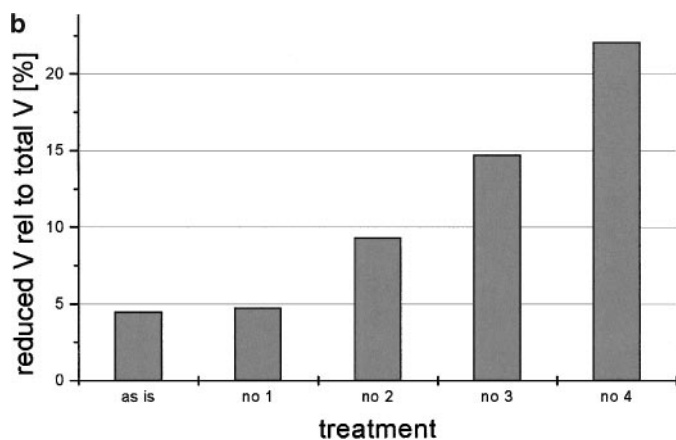
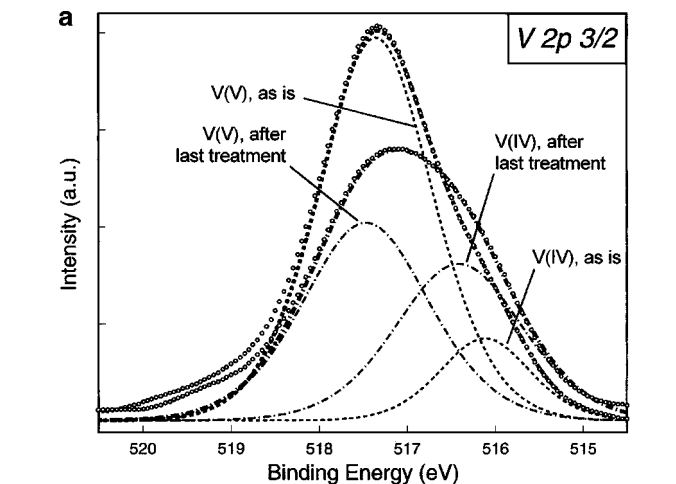


FIG. 8. (a) XPS—V (2p 3/2) peak—Shown are the least squares fits (bold lines) together with the original data (open circles); dashed lines: sample as is; dash-pointed lines: sample after last treatment; the bold lines are the sum the of two functions representing V in the oxidation levels (+V) and (+IV); (b) XPS—Relative amount of reduced V (+IV) in the catalyst after the subsequent treatment; the quantification is based on the least square fits for Fig. 7b.

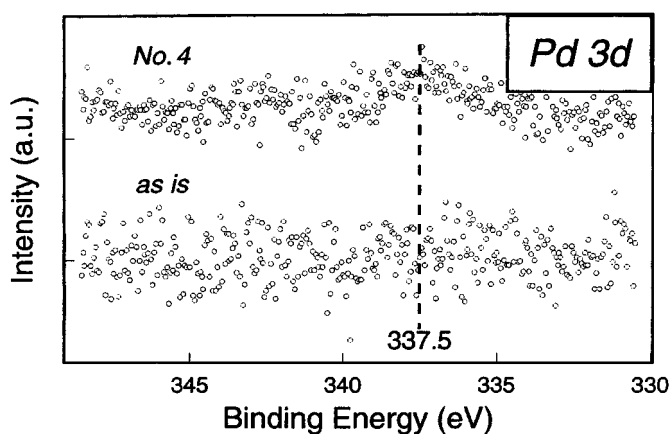


FIG. 9. XPS results, Pd (3d) region of the spectra; shown are the untreated sample (as is) and the sample after the last treatment (no. 4).

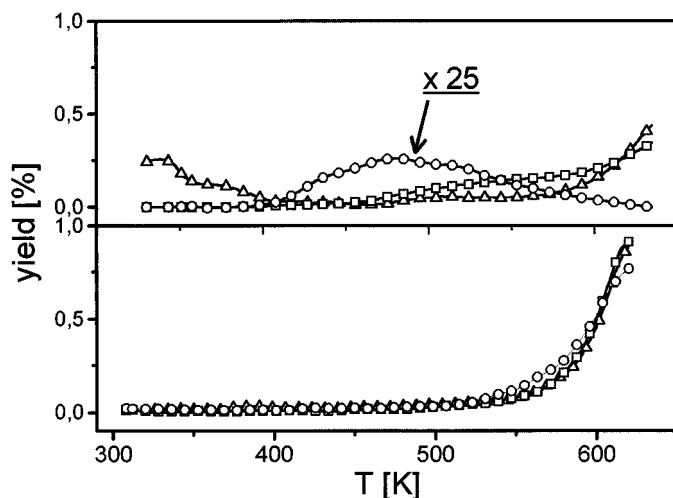


FIG. 10. TPRS—Oxidation of ethane and ethylene; yield of the main products as a function of the reactor temperature (triangles: H_2O ; squares: CO_2 ; cycles: HOAc). Upper part: ethane-TPRS (the HOAc signal is multiplied by a factor of 25 for sake of clarity) heating rate 5 K/min; atmosphere: 10% ethane and 10% oxygen in nitrogen; pressure: 100 kPa; total flow 110 ml/min. Lower part: ethylene TPRS heating rate 5 K/min; atmosphere: 5% ethylene and 20% oxygen in nitrogen; total flow 110 ml/min.

with an approximate diameter of 500 pm, the desorbed quantity would cover an area of 1.5 m^2 . The surface area of the catalyst sample is about $9 \text{ m}^2 \text{ g}^{-1}$, as determined by BET measurement. The desorbed amount of ethane is, thus, on the order of monolayer coverage.

To elucidate the mechanism of oxygen activation, transient experiments in vacuum (TAP) were carried out. In order to gain information on oxygen adsorption on the oxidised catalyst surface and oxygen exchange between gas phase and oxidised catalyst surface, a gas mixture $^{18}\text{O}_2/\text{Ne}$

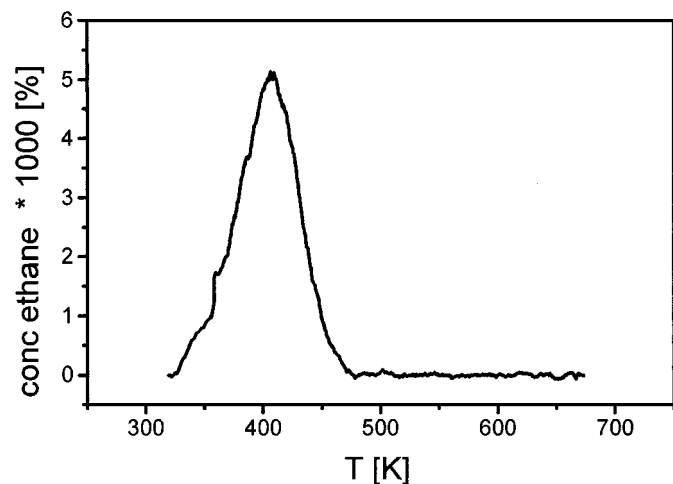


FIG. 11. TPD—Ethane: Desorption profile of ethane from the catalyst sample at atmospheric pressure after ethane adsorption from 5% ethane in nitrogen at room temperature for 5 min, heating rate 5 K/min; 100 mg of catalyst sample in a stream of 100 ml nitrogen/min.

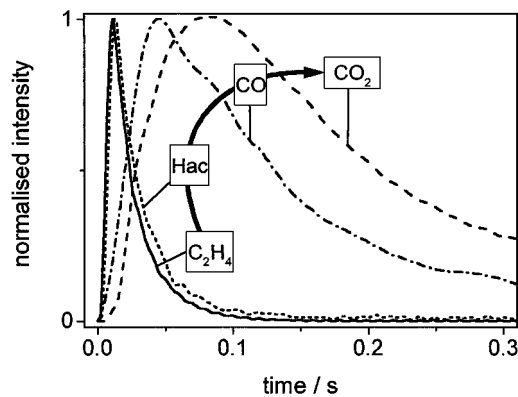


FIG. 12. Normalised signals of ethylene/Ne (1 : 1) pulses over 210 mg catalyst in TAP-reactor at 570 K (conversion of ethylene: $X_{C_2H_4} = 19\%$, selectivities: $S_{CO_2} = 23\%$, $S_{CO} = 25\%$; $S_{Hac} = 52\%$).

(1 : 1) was pulsed over the catalyst at $T = 539$ K. The response signal for $^{18}O_2$ revealed exactly the same shape as the response signal of neon except the shift caused by different Knudsen diffusion coefficients of both molecules. Oxygen exchange products like $^{18}O^{16}O$ or $^{16}O_2$ were not detected. That is, neither adsorption nor activation takes places on the oxidised catalyst.

Further TAP-experiments were carried out with ethylene. In the oxidation of ethylene under pressure (see below), a strong dependence of the reaction rate on water partial pressure was observed. Thus, experiments under vacuum at minimised water partial pressure are of interest. At $T = 573$ K a 1 : 1 ethylene/neon mixture was pulsed over the catalyst. The normalised responses for ethylene and the reaction products acetaldehyde, carbon monoxide, and carbon dioxide are shown in Fig. 12. The shapes and the shift of the pulse responses of the ethylene oxidation indicate that acetaldehyde, carbon monoxide, and carbon dioxide are formed in a consecutive reaction. The results are different from the results of the ethylene oxidation in the TPRS reactor system. Acetic acid was not detected; on the contrary, acetaldehyde (Hac) and carbon monoxide were formed being trace products in TPRS experiments. Since CO_x is formed in the absence of gas phase oxygen we can conclude that lattice oxygen is involved in unselective oxidation of ethylene. Additional experiments using pulses of $C_2H_4/O_2/Ne$ or $C_2H_4/H_2O/O_2/Ne$ did not result in detectable amounts of acetic acid or in an increase of ethylene conversion. Thus, the presence of oxygen or water in the pulses did not influence the ethylene oxidation under vacuum.

3.2. Catalysis under Conditions Close to Practise

The oxidation of ethane was investigated at different temperatures, different water partial pressures, and varying space-times to analyse the influence of operating conditions on conversion and selectivity and to elucidate the

reaction scheme. An overview of the reaction conditions is given in Table 1. Additional experiments with co-feed of a reaction product, ethylene as well as acetic acid, were performed to study the product's influence on the conversion of ethane or its activity for unselective oxidation to carbon oxides. The oxidation of ethylene to acetic acid which is an important reaction in the oxidation of ethane was studied at different temperatures and water partial pressures (see Table 1).

In the catalytic oxidation of ethane over $Mo_1V_{0.25}Nb_{0.12}Pd_{0.0005}O_x$ the most important byproduct besides the main products acetic acid, ethylene, and carbon dioxide was acetaldehyde (selectivity less than 1%). Further trace products formed in the reaction were ethyl acetate, acetone, methanol, methane, propylene, and ethanol. Carbon monoxide was not detected in the temperature range studied. Due to the low concentration of the trace products they are neglected in our further presentation.

Dependence of product selectivities on degree of conversion (without water added to feed gas). The dependence of product selectivities on the degree of conversion was studied by varying the contact time. The resulting selectivities are shown as a function of ethane conversion in Fig. 13. It can be seen that the selectivity to acetic acid and ethylene strongly changes with increasing ethane conversion while the selectivity to carbon dioxide only slightly increases from approximately 15% at the lowest ethane conversion to 20% at 2.5% ethane conversion. The selectivity to ethylene falls from approximately 85% with increasing ethane conversion to 2% at an ethane conversion of 2.5%. On the contrary, the selectivity to acetic acid increases with ethane conversion from 20%, which is the lowest selectivity found with detectable amounts of acetic acid to 80%.

These results indicate that ethylene is formed as the primary product in the oxidation of ethane and is consecutively converted to acetic acid. Carbon dioxide is as well a primary product since it is formed with significant selectivity even at the lowest degree of conversion measured ($X_{C_2H_6} = 0.14\%$). The increase in selectivity to carbon dioxide with conversion shows that ethylene and/or acetic acid are partially converted to carbon dioxide. This was further clarified in

TABLE 1
Overview of Reaction Conditions

	Ethane oxidation	Ethylene oxidation
T/K	503–576	443–520
$p_{C_2H_6}/p_{C_2H_4}/kPa$	600–650	10–30
p_{O_2}/kPa	120–130	120
p_{H_2O}/kPa	0–320	0–300
$\tau_m/10^3 \text{ kg} \cdot \text{s} \cdot \text{m}^{-3}$	1.5–65	1.15–9.8

Note. Temperature T , partial pressures p_i , modified contact time τ_m .

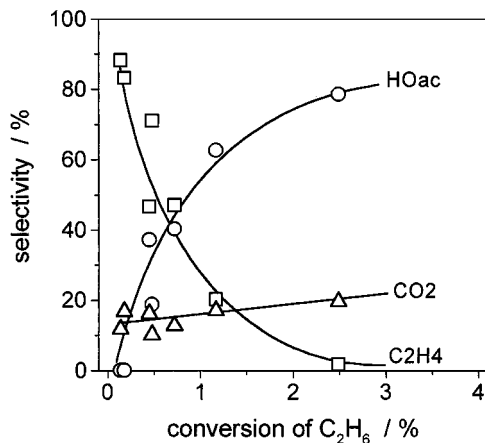


FIG. 13. Product selectivities as a function of ethane conversion without water added to the feed ($T = 503$ K, $\tau_{m,RTP} = (1.5 \text{ to } 65) \cdot 10^3 \text{ kg}_{\text{cat}} \text{ s m}^{-3}$, $p_{\text{C}_2\text{H}_6} = 650$ kPa, $p_{\text{O}_2} = 130$ kPa, $P = 1.3$ MPa).

experiments with ethylene or acetic acid respectively in the feed (see below).

Influence of water concentration in the feed on product distribution. The influence of water addition to the feed on product distribution was studied at $T = 519$ K and constant partial pressures of ethane and oxygen. The partial pressure of water was varied at constant total pressure $P_{\text{tot}} = 1.5$ MPa which was achieved by partially replacing nitrogen by water vapour in the feed.

The conversion of ethane as well as the yield of acetic acid and ethylene are shown in Fig. 14 as a function of water partial pressure at the reactor inlet. The conversion of ethane increases from 4.0% without water up to 4.7% at $p_{\text{H}_2\text{O},\text{in}} = 0.1$ MPa and then decreases gradually when the partial pressure of water is further increased. The yield

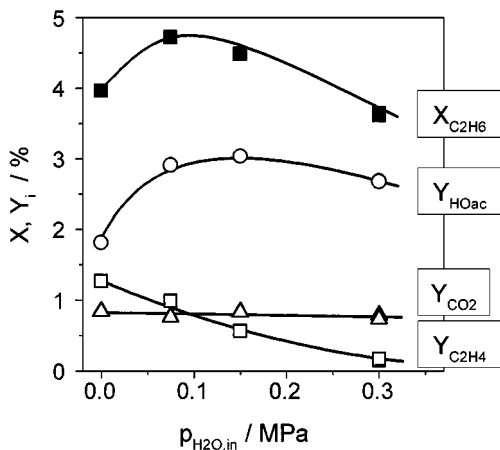


FIG. 14. Conversion of ethane and product yields as a function of water partial pressure at reactor inlet ($T = 519$ K, $\tau_{m,RTP} = 19.6 \cdot 10^3 \text{ kg s} \cdot \text{m}^{-3}$, $m_{\text{cat}} = 6.0$ g, $p_{\text{C}_2\text{H}_6} = 6.0$ bar, $p_{\text{O}_2} = 1.2$ bar, $P = 1.5$ MPa).

of ethylene decreases with increasing water partial pressure while the yield of acetic acid shows a weakly marked maximum at approximately 0.15 MPa which corresponds to $Y_{\text{HOAc}} = 3.0\%$. Comparing the selectivity values the role of water becomes clearer. While the selectivity to ethylene drops from 32% without water to 4% at $p_{\text{H}_2\text{O},\text{in}} = 0.3$ MPa, the selectivity to acetic acid rises from 45 to 74%. The yield of carbon dioxide is nearly independent of the water partial pressure.

It must be emphasised that water itself is a reaction product. Thus, the oxidation of ethane might be an autocatalytic reaction with respect to water.

On the other hand, the decrease in ethane conversion found in Fig. 14 at a high partial pressure of water accompanied by a high partial pressure of acetic acid could be attributed to adsorption of either water or acetic acid which might block active sites on the catalyst and thereby decrease the rate of ethane oxidation.

To elucidate whether ethane oxidation rate is diminished by adsorption of acetic acid, experiments with acetic acid added to the feed were performed (see below).

Dependence of product formation on contact time at different temperatures and different concentrations of water in the feed. The aim of these experiments was to gain further insight into the reaction scheme and to obtain a data basis for kinetic modelling which is described in the second part of the series (23).

Several experiments were carried out at different contact times while keeping the inlet composition constant. Three different inlet compositions were studied at two temperature levels ($T = 503$ and 576 K); the results are shown in Fig. 15.

The change in selectivity with ethane conversion described in Fig. 13 is reflected in Fig. 15a as well. At small contact time and, thus, low ethane conversion, ethylene is formed with high selectivity as a main product of ethane oxidation and reaches a maximum of 2.5 kPa at $10 \dots 15 \cdot 10^3 \text{ kg s m}^{-3}$. At higher contact times and thus higher ethane conversion, acetic acid becomes the main product while the partial pressure of ethylene decreases strongly. In contrast to that, the experiments at 503 K with water added to the feed (Figs. 15b and 15c) do not clearly indicate a consecutive reaction with ethylene as intermediate. Acetic acid and carbon dioxide are formed as main products; ethylene is only formed in traces ($S_{\text{C}_2\text{H}_4} < 2\%$). This might be due to the faster reaction of ethylene to acetic acid due to the presence of water which results in reduced selectivity to the intermediate product ethylene as discussed in Section 3.2.

The effect of water on the rate of ethane conversion observed at $T = 519$ K (Fig. 14) can be found for a lower reaction temperature of 503 K as well (Figs. 15a–15c). The converted amount of ethane, calculated as the sum of ethylene plus acetic acid plus half of carbon dioxide, is highest

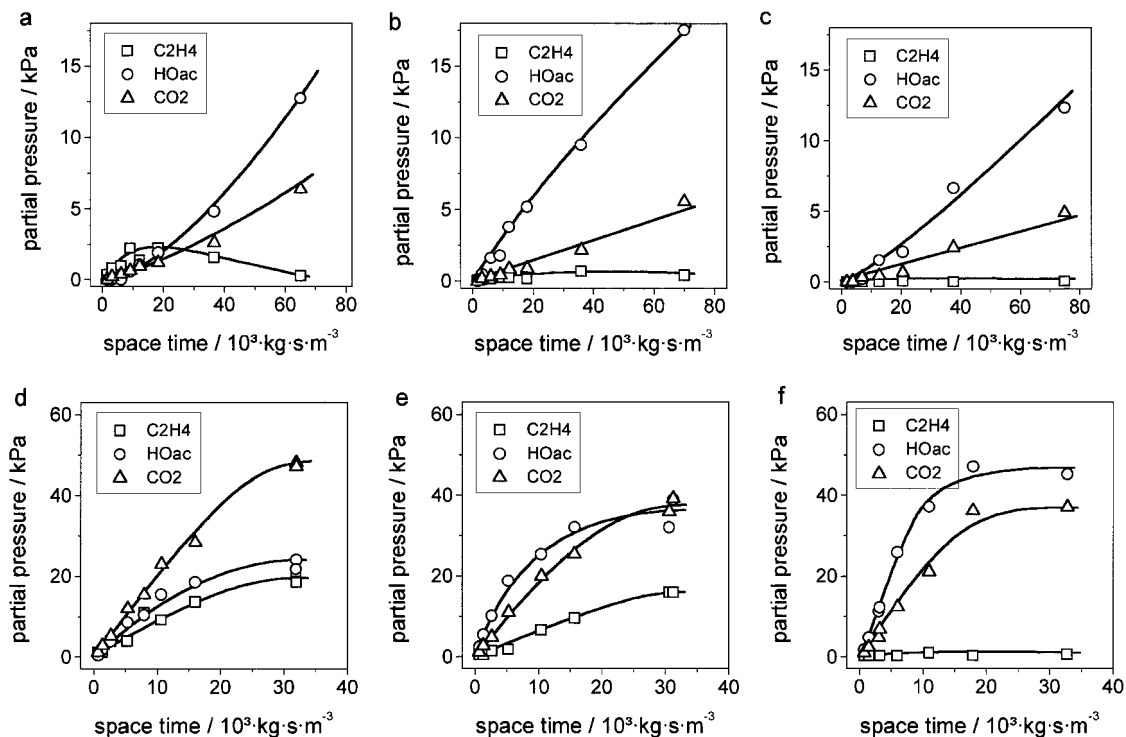


FIG. 15. Partial pressures of reaction products as a function of space–time for two different temperatures and three different water partial pressures at reactor inlet; from left to right: $p_{\text{H}_2\text{O},\text{in}} = 0/108/320$ kPa ($P_{\text{tot}} = 1.3/1.4/1.6$ MPa, respectively; $p_{\text{O}_2\text{H}_6,\text{in}} = 640 \dots 650$ kPa; $p_{\text{O}_2,\text{in}} = 128 \dots 130$ kPa); top: $T = 503$ K, bottom: $T = 576$ K.

at 503 K, $p_{\text{H}_2\text{O}} = 108$ kPa (Fig. 15b). Comparing Figs. 15a and 15c with 15b, the positive effect of water on the oxidation of ethane at low water partial pressures becomes obvious as well as the negative effect at high water partial pressures.

In contrast to the experiments at 503 K, quite different results were obtained at the high temperature $T = 576$ K (see Figs. 15d–15f) with respect to the reaction scheme. Without water in the feed, ethylene, acetic acid, and carbon dioxide are formed in parallel (Fig. 15d). The occurrence of the consecutive reaction pathway from ethane to acetic acid which could be clearly seen at the lower temperature is now totally covered up by the parallel reaction of ethane to ethylene and of ethane to acetic acid. Thus, a strong temperature dependency of different reaction pathways exists which causes this apparent shift from consecutive to parallel formation of ethylene and acetic acid.

At the medium water partial pressure and at $T = 503$ K, ethylene is formed with low selectivity (Fig. 15b). In contrast to that, at $T = 576$ K (Fig. 15e), the diminished ethylene selectivity and thereby high acetic acid selectivity was only found if the highest water partial pressures in the feed were applied ($p_{\text{H}_2\text{O},\text{in}} = 320$ kPa, Fig. 15f). From the results obtained, it follows that at the higher temperature more water is necessary to decrease ethylene selectivity and thereby increase the acetic acid selectivity to the same extent.

Oxidation of ethane/acetic acid mixtures. The reaction of an ethane/acetic acid mixture with oxygen over $\text{Mo}_1\text{V}_{0.25}\text{Nb}_{0.12}\text{Pd}_{0.0005}\text{O}_x$ was studied to analyse first whether acetic acid is converted to carbon dioxide and second whether acetic acid inhibits the oxidation of ethane.

The results of the two experiments carried out are shown in Table 2. Ethane was oxidised with oxygen in the presence of water first without adding acetic acid to the feed. Then nitrogen was partially replaced by acetic acid. In the experiment with acetic acid in the feed, 1.5 times more carbon dioxide was formed, which shows that acetic acid is partially

TABLE 2

Effect of Co-Feeding Acetic Acid on Conversion of Ethane and Yields to Main and Trace Products

$p_{\text{HOac},\text{in}}/\text{kPa}$	0	26
$X_{\text{C}_2\text{H}_6}/\%$	3.47	3.51
$Y_{\text{HOac}}/\%$	2.41	1.97
$Y_{\text{C}_2\text{H}_4}/\%$	0.075	0.069
$Y_{\text{CO}_x}/\%$	0.96	1.42
$Y_{\text{CH}_3\text{OH}}/\%$	0.003	0.006
$Y_{\text{Hac}}/\%$	0.003	0.003
$Y_{\text{acetone}}/\%$	0.009	0.024
$Y_{\text{acOet}}/\%$	0.010	0.023

Note. $T = 540$ K; $p_{\text{C}_2\text{H}_6} : p_{\text{O}_2} : p_{\text{H}_2\text{O}} : (p_{\text{HOac}} + p_{\text{N}_2}) = 600 : 120 : 300 : 480$ kPa; $m_{\text{cat}} = 6.0$ g, $\tau_{\text{m,RTP}} = 9.8 \cdot 10^3$ kg \cdot s \cdot m $^{-3}$.

converted to carbon dioxide. As mentioned in the experimental section, degradation of acetic acid due to noncatalytic reactions can be ruled out.

The amount of ethane converted was not influenced by the addition of acetic acid. In Section 3.2, it could not be distinguished whether the decrease in the ethane conversion at high water partial pressures (Fig. 14) is due to blocking of sites by water or by acetic acid. Since acetic acid does not influence the amount of ethane converted the decrease in ethane conversion can be attributed to water adsorption.

When adding acetic acid to the feed higher amounts of the trace products methanol, acetone, and ethyl acetate (acOet) were formed indicating that acetic acid participates in their formation. Formation of acetaldehyde (Hac) is independent of co-feeding acetic acid.

Oxidation of ethylene and of ethane/ethylene mixtures. The oxidation of ethylene as well as of ethane/ethylene mixtures over $\text{Mo}_1\text{V}_{0.25}\text{Nb}_{0.12}\text{Pd}_{0.0005}\text{O}_x$ was studied to confirm the postulated strong influence of water on the oxidation of ethylene to acetic acid. Again, different inlet water partial pressures were applied.

The results of the oxidation of ethylene at $T = 520$ K for three different inlet water partial pressures are summarized in Table 3. All experiments were carried out at the same space–time with stoichiometric excess of oxygen ($\text{C}_2\text{H}_4 : \text{O}_2 = 1 : 12$). Different partial pressures of water at constant total pressure were achieved by replacing nitrogen partially with water while the total gas flow was kept constant. The conversion of ethylene without water in the feed was $X_{\text{C}_2\text{H}_4} = 18.9\%$ and increased to $X_{\text{C}_2\text{H}_4} = 77.2\%$ at an inlet water partial pressure of 50 kPa. A further increase of water partial pressure at the reactor inlet to 200 kPa resulted in nearly complete conversion of ethylene ($X_{\text{C}_2\text{H}_4} = 99.4\%$). Adding water to the feed also increased the selectivity to acetic acid from 73.3 to 92.9%. This is an unusual behaviour for selective oxidation reactions since the selectivity to the partial oxidation product usually decreases with increasing conversion of the hydrocarbon.

TABLE 3

Degree of Ethylene and Oxygen Conversion ($X_{\text{C}_2\text{H}_4}$, X_{O_2}), Selectivities (S_i), and Space–Time Yields (STY) of Acetic Acid in the Oxidation of Ethylene with Molecular Oxygen at Different Water Partial Pressures in the Feed Gas

$p_{\text{H}_2\text{O, in}}/\text{kPa}$	0	50	200
$X_{\text{C}_2\text{H}_4}/\%$	18.9	77.2	99.4
$X_{\text{O}_2}/\%$	1.8	7.6	9.9
$S_{\text{HOAc}}/\%$	73.3	88.8	92.9
$S_{\text{CO}_x}/\%$	23.8	10.4	6.8
$\text{STY}_{\text{HOAc}}/\text{g}_{\text{HOAc}} \text{ kg}^{-1} \text{ h}^{-1}$	60.2	298	401

Note. Taken at $T = 520$ K, $p_{\text{O}_2} : p_{\text{C}_2\text{H}_4} : (p_{\text{H}_2\text{O}} + p_{\text{N}_2}) = 120 : 10 : 400$ kPa; $m_{\text{cat}} = 2.03$ g, $\tau_m = 1.15 \cdot 10^3$ kg \cdot s \cdot m $^{-3}$.

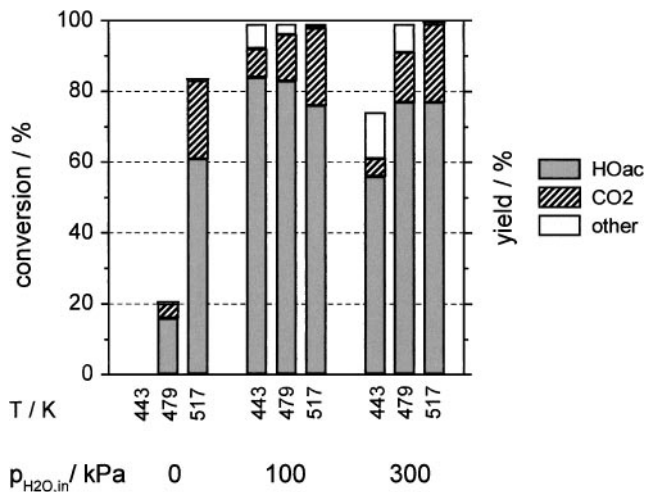


FIG. 16. Conversion of ethylene in the oxidation of ethane/ethylene mixtures with oxygen at different temperatures and partial pressures of water in feed gas; conversion calculated ($p_{\text{C}_2\text{H}_6} : p_{\text{C}_2\text{H}_4} : p_{\text{O}_2} = 600 : 30 : 120$ kPa; $m_{\text{cat}} = 6.0$ g; $\tau_{m, \text{RTP}} = (11.72/10.83/10.03) \cdot 10^{-3}$ kg \cdot s \cdot m $^{-3}$ at $T = 443/479/517$ K, respectively).

In order to analyse whether the results of the ethylene oxidation experiments are still valid in high excess of ethane, some experiments were carried out with ethane/ethylene mixtures. Again the water partial pressure was varied. The space–time, which was held constant for all experiments, was increased compared to the experiments with ethylene only. Lower reaction temperatures of 443, 479, and 517 K were chosen, since the previous results had shown that the reaction of ethylene is much faster than the reaction of ethane. The results from studying the conversion of mixtures of ratio ethane : ethylene = 20 : 1 at varying water partial pressures in the feed gas ($p_{\text{H}_2\text{O, in}} = 0/100/300$ kPa) and different temperatures are shown in Fig. 16. The conversion of ethylene was calculated under the assumption that ethane is not reacting at these temperatures which is true for $T = 443$ and 479 K and an approximation for $T = 517$ K. The essential role of water on the oxidation of ethylene to acetic acid is underlined by the results obtained: At $T = 443$ K, a conversion of ethylene was not found without water in the feed. However, already an inlet water partial pressure of 100 kPa resulted in complete conversion of ethylene even at the lowest temperature. An increase of inlet water partial pressure to 300 kPa reduced the conversion of ethylene as well as the yield of acetic acid. These results show that there is an optimum value for the partial pressure of water in the ethylene oxidation. This is comparable to the ethane oxidation where an optimum for the partial pressure of water was found as well (Fig. 14). The other products formed were acetaldehyde, ethyl acetate, acetone, methanol, and ethanol. The formation of these byproducts increases with decreasing temperature and increasing water partial pressure. In the experiments with ethylene and with

ethylene/ethane mixtures stronger temperature gradients (>10 K) appeared than in the oxidation of ethane alone although the catalyst was diluted with quartz as before.

It is interesting to note that in the steady-state experiments significantly lower selectivities to CO_x were found compared to the TAP experiment ($S_{\text{CO}_x} = 48\%$). For activity as well, a strong difference was observed. In the ethylene oxidation under pressure a very high activity at temperatures as low as 443 K was found. In contrast, in TAP reactor under vacuum a much higher temperature was necessary (573 K) to achieve significant conversion. At atmospheric pressure in the TPRS equipment a temperature somewhere in between (approximately 500 K), was found where ethylene oxidation started. The comparison of TAP and steady-state results clearly indicates that the presence of water and/or oxygen in the gas phase is necessary to convert ethylene to acetic acid effectively and selectively.

4. DISCUSSION

The following discussion is focussed on (i) the mechanism of the catalytic reaction and (ii) optimised conditions for maximising the yield and selectivity of acetic acid.

4.1. Reaction Scheme

According to Thorsteinson *et al.* (4), the formation of acetic acid occurs as a consecutive reaction with ethylene as intermediate; the formation of CO_x is considered by Thorsteinson (4) as an unselective oxidation step of ethylene. Oxidation of ethane or acetic acid to CO_x was not considered. In contrast to Thorsteinson's findings, the dependency of the carbon dioxide selectivity on the ethane conversion shows that carbon dioxide has its origin most probably not only in ethylene, since in our experiments even at the lowest ethane conversions at which carbon dioxide was detectable its selectivity is still significant (ca 15%, see Fig. 13). Thus, most probably carbon dioxide is partially also formed by direct oxidation of ethane over the present catalyst. In addition, the experiments with co-feed of acetic acid showed that the total oxidation of acetic acid contributes to carbon dioxide formation as well.

The results from TPRS measurements at atmospheric pressure support the assumption of a consecutive mechanism for the oxidation of ethane with ethylene as an intermediate. The ethane TPRS shows a weak maximum for acetic acid centred at 500 K and a plateau for water and carbon dioxide formation from 500 to 600 K. Furthermore, in the ethane-TPRS, acetic acid has completely disappeared above 600 K. At this temperature, the water and carbon dioxide yields rise exponentially. This fact is in agreement with a consecutive oxidation of acetic acid, leading to complete elimination of this compound at higher temperatures. Considering the ethane- and ethylene-TPRS, it is obvious

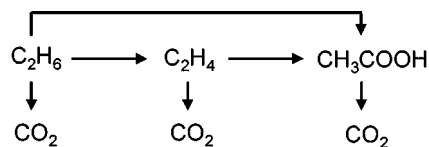


FIG. 17. Reaction scheme for the oxidation of ethane to acetic acid.

that the oxidation of ethane proceeds not over ethylene exclusively. Otherwise, acetic acid would not disappear at higher temperatures in the oxidation of ethane but would show the same behaviour as in that of ethylene-TPRS. The reduced acetic acid yield relative to that of carbon dioxide and water in the ethylene TPRS thus results from the oxidation of acetic acid.

Based on the results, a simple reaction scheme for the oxidation of ethane was developed (Fig. 17). This scheme includes a parallel reaction of ethane to ethylene and acetic acid as well as a consecutive reaction to acetic acid with ethylene as intermediate. Carbon dioxide can be formed by unselective oxidation of ethane, ethylene, and acetic acid. The observed change in the reaction path with increasing temperature implies different apparent energies of activation for the direct formation of acetic acid from ethane preferred at high temperature and the formation via ethylene preferred at low temperature. That is, the activation energy of the oxidation of ethane to ethylene has to be lower than the activation energy of the direct oxidation of ethane to acetic acid. More detailed information on the properties of the active sites for the particular reaction steps are given in the following paragraphs.

4.2. Mechanism

Activation of oxygen. The oxygen pulse experiments have shown that oxygen adsorption did not take place on the oxidised catalyst surface. Thus, for the present catalyst a Mars–VanKrevelen type redox reaction is suggested as mechanism. The catalyst is reduced during reaction and re-oxidised by gas phase oxygen. This mechanism has been suggested on the Mo-V-Nb-O catalyst without palladium by several authors (4, 7, 25).

Weakly bound oxygen species, which are supposed to be responsible for unselective oxidation (26), do not exist on the catalyst surface as indicated by the oxygen-pulse experiments. Thus, unselective oxidation must be attributed to lattice oxygen as well. This was confirmed in the ethylene pulse experiment in which CO_x was formed without oxygen being present in gas phase.

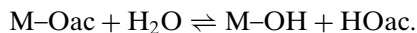
As indicated by the XPS analysis, vanadium is the redox centre of the $\text{Mo}_1\text{V}_{0.25}\text{Nb}_{0.12}\text{Pd}_{0.0005}\text{O}_x$ catalyst since only for vanadium a change of the oxidation state was observed after treatment with ethylene oxygen mixtures but not for the molybdenum. By XRD vanadium containing phases were not observed. Since the Mo_5O_{14} structure which was

identified by XRD is known to tolerate partial substitution of molybdenum by vanadium as already shown earlier by Khilborg (27) and the Mo_5O_{14} phase seems to serve only as host structure stabilising the vanadium redox centres.

Activation of ethane. Hard acid cations as V^{4+} or V^{5+} linked to oxygen are necessary on the surface of the catalyst to activate ethane (4, 5). After adsorption of ethane as ethoxide, ethylene may be formed by β -hydrogen abstraction. Ethane exhibits only weak interaction with the catalyst surface, as shown by the ethane TPD experiment, complete desorption occurred below 500 K. Above the minimum temperature for lattice oxygen to become active (ca. 500 K), the coverage of the catalyst surface by ethane would be very low unless high ethane partial pressures are applied. Under atmospheric pressure and a partial pressure of ethane in the range of 10 kPa, there is no overlap of the temperature region in which the catalyst is still covered by ethane and the temperature region in which the lattice oxygen becomes active. In principle, the optimum working temperature of the present catalyst will be determined by the maximum overlap of adsorption and oxygen activity. With rising ethane partial pressure, this overlap increases and the optimum temperature will shift to higher values. Thus, the oxidation of ethane has to be carried out at high partial pressures of ethane in order to achieve acceptable space–time yields.

Mechanistic interpretation of water effect in ethane and ethylene conversion. A different influence of water was observed for the oxidation of ethane and the oxidation of ethylene with respect to the formation of carbon dioxide: Ethane as well as ethylene oxidation are accelerated by the presence of water up to a certain maximum, whereas the rate of carbon dioxide formation remains nearly constant regardless of the water partial pressure. Thus, to explain the influence of water, at least two catalytic centres must be assumed, which differ in the way they are affected by water. In the second part of the series two kinetic models were suggested each considering two different catalytic centres (23). The drop of reaction rate for ethane as well as ethylene oxidation above the maximum may be attributed to competitive adsorption of water on catalytically active sites where ethylene or ethane respectively are activated or where catalyst reoxidation takes place.

According to Tessier *et al.* (9) water displaces adsorbed acetic acid from the active centre



This desorption is considered to be rate determining for VO_x and VPO catalysts supported on TiO_2 . This explanation for the effect of water implies that the maximum rate of acetic acid formation is determined by the partial pressure of water. Thus, no matter if ethane or ethylene is oxidised the space–time yield of acetic acid should be

approximately the same. For the $\text{Mo}_1\text{V}_{0.25}\text{Nb}_{0.12}\text{Pd}_{0.0005}\text{O}_x$ catalyst the space–time yield for acetic acid at complete oxygen conversion in the oxidation of ethane is much lower ($37 \text{ g}_{\text{HOac}}/\text{kg}_{\text{cat}}/\text{h}$) at $T = 539 \text{ K}$ than the space–time yield of acetic acid in the oxidation of ethylene which amounts to $400 \text{ g}_{\text{HOac}}/(\text{kg}_{\text{cat}} \cdot \text{h})$ at $T = 520 \text{ K}$ as shown in Table 3. Thus, Tessier's explanation for the effect of water cannot be adapted to the $\text{Mo}_1\text{V}_{0.25}\text{Nb}_{0.12}\text{Pd}_{0.0005}\text{O}_x$ catalyst, since different space–time yields of acetic acid were obtained in the experiments with ethane and ethylene at comparable water partial pressures.

Therefore, a different mechanism for the accelerating effect of water on the rate of ethane oxidation has to be discussed. We suspect that the rate of ethane oxidation is indirectly accelerated when the rate of ethylene oxidation increases. This may be caused by adsorption of ethylene on sites involved in the oxidation of ethane. Thus, at high ethylene partial pressures, which are linked to low water partial pressures, the ethane oxidation is slowed down due to the blocking of sites by ethylene. Increasing the water partial pressure leads to faster conversion of ethylene to acetic acid and thereby indirectly to an increase of the ethane oxidation rate, since less sites are blocked by ethylene. This idea was proven to be successful in our modelling of the kinetics of the oxidation of ethane to acetic acid, as reported elsewhere (23).

Acetic acid formation—role of palladium. The strong influence of water on the oxidation of ethylene to acetic acid has been known from the literature for the heterogeneous Wacker oxidation of ethylene to acetaldehyde and/or acetic acid which has been performed on, e.g., Pd-doped vanadium(V)oxide (18, 19). As noted in the previous section the accelerating effect of water cannot be explained by water-induced desorption of acetic acid. Thus, the accelerating effect of water is attributed to the formation of hydroxyl groups in the present work. The hydroxyl groups are supposed to participate in the rate determining step of the heterogeneous Wacker oxidation (19, 28). It is supposed that acetaldehyde is formed first as intermediate, which is indicated by pulse experiments with ethylene (Fig. 12). Acetaldehyde is then rapidly further oxidised to acetic acid either by gas phase oxygen or lattice oxygen. Indirect evidence for the importance of hydroxyl groups results from the low rate of ethylene oxidation found in the vacuum pulse experiment, which can be attributed to the removal under vacuum of HO centres, which are essential for the Wacker oxidation.

At the highest temperature ($T = 576 \text{ K}$), more water is necessary to convert ethylene to acetic acid than at the lower temperatures (see Fig. 15). This may be due to a decrease in the concentration of the OH sites active for Wacker oxidation with increasing temperature.

These results point to the role palladium might play in the catalyst. As known from the literature the presence

of palladium is necessary to perform an efficient heterogeneous Wacker oxidation. Compared to the Pd-free analogue $\text{Mo}_1\text{V}_{0.25}\text{Nb}_{0.12}\text{O}_x$, the present catalyst showed much higher selectivity to acetic acid of typical $S_{\text{HOAc}} = 80\%$ compared to 26% reported by Thorsteinson *et al.* for the Pd-free catalyst (4). Thus, we believe that the addition of palladium introduced catalytic activity for Wacker oxidation in the $\text{Mo}_1\text{V}_{0.25}\text{Nb}_{0.12}\text{O}_x$ catalytic system, which makes it possible to convert the intermediate ethylene effectively to acetic acid. In this way, the increase of acetic acid selectivity at the expense of ethylene selectivity is explained.

From the catalyst characterisation by SEM/EDX and XPS the following information on the state of palladium can be deduced. Since the palladium concentration was near the detection limit of SEM/EDX it can be concluded that palladium should be highly dispersed. Palladium was not found by XPS analysis in the samples “as is” and after low temperature treatment ($T = 523\text{ K}$) by ethylene/oxygen mixture. This indicates that palladium is dispersed in the bulk. Only after the treatment at 623 K a very weak Pd(3d) signal was observed indicating that palladium becomes mobile. A migration of Pd species to the surface occurred. The state of the palladium species does not correspond to a metallic one but rather to Pd(II). From Pd supported on MgO it is known that a migration of palladium occurs already at a temperature of 400 K (29, 30). In the present catalytic system palladium migration occurs at higher temperature. Presumably, the Mo_5O_{14} like structure is able to stabilise palladium in its dispersive state. Thus, this structure might serve not only as a host for vanadium and niobium but also for the palladium. The stabilisation of the oxidation state Pd(II) is connected to the high dispersion. Since metallic palladium is known as combustion catalyst, the high selectivity to acetic acid of the $\text{Mo}_1\text{V}_{0.25}\text{Nb}_{0.12}\text{Pd}_{0.0005}\text{O}_x$ catalyst should be possible due to the presence of nonmetallic palladium. This corresponds to the idea discussed above that palladium acts as a Wacker catalyst.

4.3. Optimised Conditions for Producing Acetic Acid

The most pronounced effect of water was observed in the experiments carried out with ethylene present in the feed (Table 1, Fig. 16). The experimental results of the oxidation of both the ethylene and ethane/ethylene mixtures show that the rate of ethylene oxidation increases with increasing water partial pressure up to a maximum. Thus, an optimum value for water partial pressure exists at which the acetic acid yield reaches a maximum. However, water on the one hand increases selectivity, but on the other hand it causes higher costs in concentrating the more diluted acetic acid in an industrial process.

To obtain space–time yields of acetic acid sufficiently high for an industrial process, the catalyst has to be operated at a higher temperature (approximately $T > 550\text{ K}$). However,

an enhancement of the process temperature is limited by the metastable character of the Mo_5O_{14} phase, wherein the active vanadium species as well as Pd(II) are located. This phase is irreversibly transformed above 600 K. To achieve high selectivity to acetic acid at higher temperature, more water is needed than at lower temperature. Thus, increasing space–time yield by increasing the temperature has the drawback of requiring higher water concentration to maintain high selectivities to acetic acid. As already pointed out water is disadvantageous in the chemical process of ethane oxidation to acetic acid since the energy consumption in the separation stages increase strongly with water concentration.

The following discussion is focussed on the rate determining steps for acetic acid formation; their identification will lead to concepts for further catalyst optimisation:

(i) At high water concentrations acetic acid is the main product; the intermediate ethylene is only formed in traces; i.e., it reacts quickly to acetic acid and/or carbon dioxide (see Figs. 15c and 15f). Thus, either ethane activation or catalyst reoxidation can be considered as rate determining steps since our results have shown that limitation by acetic acid desorption can be excluded in this context. An approximate rate of catalyst reoxidation was calculated for both experiments, the oxidation of ethane and the oxidation of ethylene: in ethane oxidation the oxygen consumption is $4.3 \cdot 10^{-4}\text{ mol} \cdot \text{s}^{-1} \cdot \text{kg}^{-1}$ at $T = 539\text{ K}$, which is clearly below the value of $2.4 \cdot 10^{-3}\text{ mol} \cdot \text{s}^{-1} \cdot \text{kg}^{-1}$ found in ethylene oxidation at even lower temperature ($T = 520\text{ K}$). Thus, catalyst reoxidation is unlikely to be a rate determining step in ethane oxidation, since the catalyst shows the potential for high reoxidation rate with ethylene; the slower reoxidation rate found in ethane oxidation is due to slow catalyst reduction by ethane. Thus, we conclude, that the activation of ethane is the rate determining step for oxidising ethane to acetic acid. A major reason may be the weak interaction of ethane with the catalyst, preventing a pronounced coverage of the surface at temperatures necessary for lattice oxygen to become active.

(ii) At low water concentrations and higher temperature, acetic acid and ethylene are the main products (see Figs. 15d and 15e). This implies that ethylene conversion to acetic acid is slow under these conditions. Therefore, under water poor conditions the rate determining step shifts from ethane activation to the conversion of ethene to acetic acid; e.g., a step in the formation of Wacker sites may be rate determining.

As a consequence, in further catalyst development, one must focus on the activation of ethane as a rate determining step to improve the space–time yield of acetic acid. Moreover, if the catalyst shall be operated at low water concentrations in an industrial process, which is preferred, it is also important to increase the rate of ethylene conversion to acetic acid at low water concentrations.

Additionally, for a further increase in selectivity, the rates of total oxidation reactions have to be reduced. This might be achieved by modifying the catalysts composition and/or certain steps of the preparation procedure, e.g., the calcination conditions.

The actual catalyst is heterogeneous on the μm scale. Most striking is the content of pure MoO_3 and the inhomogeneity of the Nb and V distributions. The desired activity for partial ethane oxidation may be linked to the appearance of the Mo_5O_{14} -phase, probably stabilised by Nb (4, 6–8), wherein the active vanadium species as well as Pd(II) species are located. Therefore, alterations of the preparation process may enhance the fraction of this phase in benefit for the partial oxidation activity.

The influence of oxygen, water, and ethane partial pressure on the oxidation of ethane and the yield to acetic acid is included in the kinetic model presented in part II of the present series (23).

5. CONCLUSIONS

The following key factors were found to be important for the oxidation of ethane to acetic acid on $\text{Mo}_1\text{V}_{0.25}\text{Nb}_{0.12}\text{-Pd}_{0.0005}\text{O}_x$: The catalytic experiments revealed a change in reaction mechanism with increasing temperature. While a consecutive reaction scheme dominates at low temperatures with ethylene as intermediate leading to acetic acid, ethylene and acetic acid are mainly formed in parallel at high temperatures. The initial step for both pathways is the reaction of ethane with lattice oxygen. This step is related to a change of the vanadium oxidation state acting as redox centre. The ethylene formed undergoes a consecutive reaction to acetic acid. The mechanism of this reaction step can be described as a heterogeneous Wacker reaction where highly dispersed Pd(II) acts as catalytic centre. The role of water in this step seems to be similar to that in the homogeneous Wacker reaction of ethylene to acetic acid; i.e., hydroxyl groups are formed due to the interaction of water with the Pd(II) leading to the active site for ethylene conversion. Following this idea, the $\text{Mo}_1\text{V}_{0.25}\text{Nb}_{0.12}\text{Pd}_{0.0005}\text{O}_x$ catalyst can be considered as an example for the transfer from a homogeneous to a heterogeneous catalyst.

The high dispersion of palladium in the present catalyst system even maintained under reaction conditions results from the incorporation of small amounts of palladium into a Mo_5O_{14} -like phase serving as host structure also for vanadium and niobium. The catalyst sample was characterized by a nonhomogeneous morphology and elemental distribution where MoO_3 was found besides Mo_5O_{14} . Since the MoO_3 phase is known to catalyze the total oxidation steps, further catalyst optimization should be focussed on the preparation techniques to avoid the formation of this undesired phase structure.

The present findings were used as basis for kinetic modelling of the oxidation of ethane to acetic acid including water as an important variable (23).

REFERENCES

- Sano, K. I., Uchida, H., and Wakabayashi, S., *Catal. Surv. Jpn.* **3**, 55 (1999).
- "Ullmann's Encyclopedia of Industrial Chemistry," 5th ed. VCH, Weinheim, 1991.
- Bañares, M. A., *Catal. Today* **51**, 319 (1999).
- Thorsteinson, E. M., Wilson, T. P., Young, F. G., and Kasai, P. H., *J. Catal.* **52**, 116 (1978).
- Merzouki, M., Taouk, B., Monceaux, L., Bordes, E., and Courtine, P., in "Stud. Surf. Sci. Catal." Vol. 72, p. 165. New Developments in Selective Oxidation by Heterogeneous Catalysis, 1992.
- Burch, R., Kieffer, R., and Ruth, K., *Topics Catal.* **3**, 355 (1996).
- Ruth, K., Burch, R., and Kieffer, R., *J. Catal.* **175**, 27 (1998).
- Merzouki, M., Taouk, B., Bordes, E., and Courtine, P. in "New Frontiers in Catalysis—Stud. Surf. Sci. Catal." (L. Guzzi *et al.*, Eds.), Vol. 75, p. 753, 1993.
- Tessier, L., Bordes, E., and Gubelmann-Bonneau, M., *Catal. Today* **24**, 335 (1995).
- Roy, M., Gubelmann-Bonneau, M., Ponceblanc, H., and Volta, J. C., *Catal. Lett.* **42**, 93 (1996).
- Hallet, C. (BP Chemicals), European Patent Application EP 0 480 594, 1992.
- Kitson, M. (BP Chemicals), U.S. Patent 5 210 293, 1993.
- Kitson, M. (BP Chemicals), European Patent Application EP 0 407 091, 1991.
- Blum, P. R., and Pepera, M. A. (Standard Oil), U.S. Patent 005 300 682, 1994.
- Borchert, H., and Dingerdissen, U. (Hoechst), Ger. Offen. DE 19 630 832, 1998.
- Borchert, H., Dingerdissen, U., and Weiguny, J. (Hoechst), Ger. Offen. DE 19 620 542, 1997.
- Borchert, H., Dingerdissen, U., and Roesky, R. (Hoechst), Ger. Offen. DE 197 17 076 A 1, 1998.
- Evvin, A. B., Rabo, J. A., and Kasai, P. H., *J. Catal.* **30**, 109 (1973).
- Seoane, J. L., Boutry, P., and Montarnal, R., *J. Catal.* **63**, 191 (1980).
- Van der Heide, E., De Wind, M., Gerritsen, A. W., and Scholten, J. J. F., in "Proceedings, 9th International Congress on Catalysis, Calgary, 1988" (M. J. Phillips and M. Ternan, Eds.), p. 1648. Chem. Institute of Canada, Ottawa, 1988.
- Nowinska, K., and Dudko, D., *Appl. Catal. A* **159**, 75 (1997).
- Espeel, P. H., Peuter, G. de, Tielen, M. C., and Jacobs, P. A., *J. Phys. Chem.* **98**, 11,588 (1994).
- Linke, D., Wolf, D., Baerns, M., Zeyß, S., and Dingerdissen, U., *J. Catal.*, doi:10.1006/jcat.2001.3368.
- Gleaves, J. T., Yablonski, G. S., Phanawadee, P., and Schuurman, Y., *Appl. Catal.* **160**, 55 (1997).
- Burch, R., and Swarnakar, R., *Appl. Catal.* **70**, 129 (1991).
- Zanthoff, H. W., Buchholz, S. A., Pantazidis, A., and Mirodatos, C., *Chem. Eng. Sci.* **54**, 4397 (1999).
- Khilborg, L., in "Non-Stoichiometric Compounds" (R. F. Gould, Ed.), Adv. Chem. Series, Vol. 39, p. 37, 1973.
- Forni, L., and Terzoni, G., *Ind. Eng. Chem. Process. Des. Dev.* **16**, 288 (1977).
- Abbet, S., Sanchez, A., Heiz, U., Schneider, W.-D., Ferrari, A. M., Pacchioni, G., and Rösch, N., *Surf. Sci.* **454**, 984 (2000).
- Abbet, S., Sanchez, A., Zeiz, U., Schneider, W.-D., Ferrari, A. M., Pacchioni, G., and Rösch, N., *J. Am. Chem. Soc.* **122**, 3453 (2000).